 https://doi.org/10.24191/jeesr.v23i1.011

Level Shifter Signal Conditioning Circuit Design for 3-electrode Cell Portable Redox Sensor

Nur Rabi'atul 'Adawiyah Muhd Zain, Zatieyl Aqmar Nordin, Aimi Bazilah Rosli and Wan Fazlida Hanim Abdullah*

***Abstract*—This paper presents the effect of level shifter signal conditioning circuits in a low-cost portable potentiostat, implemented by combining several circuit modules and controlled by Advanced RISC Machines Cortex processor. Two architectures of level shifter modules are simulated: Non-inverting Summing Amplifier and Inverting Summing Amplifier. The main objective is to improve signal detection readability by widening the input voltage signal processing and increasing the amplitude range of the sensor output signal before the analog to digital signal conversion. The potential amplitude range of redox reaction captured by trans-impedance module at -3 V to 3 V is reduced by 50%. Then, the output voltage is converted by analog digital converter to be interfaced with microcontroller for Differential Pulse Voltammetry current properties. The designed potentiostat has a current readout range of ± 500mA and is validated to be at 15% difference with the standard laboratory potentiostat.**

***Index Terms*—Differential Pulse Voltammetry, level shifter, potentiostat, signal conditioning, redox current.**

I. INTRODUCTION

ELECTROCHEMICAL sensors and biosensing allows the versatility of electrochemical methods to provide a low cost, real-time and in-situ investigation in chemical composition [1]. The characterization investigation is done by the assistance of electrochemical instrumentation known as a potentiostat. Potentiostats are widely used such as in air quality monitoring, food and beverage safety analysis, and biomedical field [2]–[11]. The functionalities of existing potentiostat equipment depends on the cost whereas a low-cost potentiometric only provided a basic specification of potentiometric[12].

This manuscript is submitted on September 13th, 2022, revised on November 15th, 2022, accepted on December 15th, 2022 and published on October 31st, 2023. NRA. M.Zain, ZA. Nordin and A.B Rosli authors are with Integrated Sensors Research Lab, School of Electrical Engineering, College of Engineering, Universiti Teknologi MARA, 40450 Shah Alam, Selangor, Malaysia (e-mail: 2017368907@student.uitm.edu.my).

W.F.H Abdullah is an Associate Professor in the Discipline of Electronics, UiTM, with research interest in microelectronics, sensor devices, interfacing circuits and systems.

*Corresponding author
Email address: wanfaz@uitm.edu.my

The study on low-cost potentiostats have been done extensively. There are many studies done on low-cost potentiostats [13]–[17]. Most of the studies focuses on minimal specification potentiostat design, architecture allowing construction using off-shelve components[6]. Point-of-Care devices is an example of low-cost potentiostat being widely used under current health scenarios. Nevertheless, most of the development of point-of-care devices focuses on chemical compounds [18]–[22].

Typically, a basic potentiostat circuit consists of 3 amplifiers as shown in Fig 1.

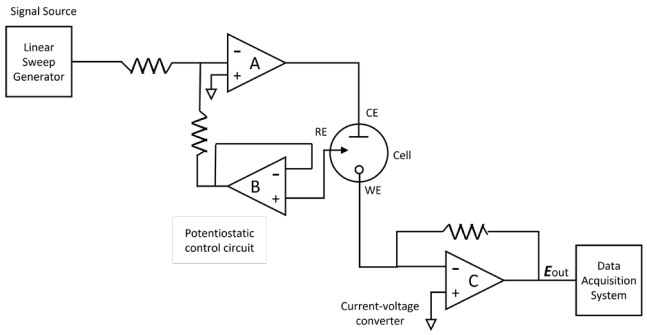

Fig. 1. Basic potentiostat circuit [23]

These amplifiers configuration is used to force current flow from counter electrode (CE) to working electrode (WE) and avoid drawback current from reference electrode RE). Then, the resulting current is recorded by data acquisition system through analog digital converter (ADC) which is the main module in it. ADC is used to interface the microcontrollers with the transimpedance to establish the differential pulse voltammetry (DPV) [19]–[22].

The resulting current which also known as redox current is small and noisy[24], [25]. It is important to retain the originality of measured signal especially when deal with low and noisy signal. Hence, researchers had proposed several signal conditioning circuit module between transimpedance and ADC stage [1], [21], [26]–[28]. In addition the implementation on signal conditioning methods before the digital stage also helps to increase the readout SNR at the cost of limited input current range due to the amplifier swing [29].Thus, it is important to consider appropriate signal conditioning circuit in designing a portable potentiostat.

The focus of this paper is on level shifter signal conditioning method for low-cost portable potentiostat circuit design based on 32-bit microcontroller. In this research work, the potentiostat design consists of a control amplifier, trans-impedance amplifier, and level shifter amplifier module that is controlled by MCU. MCU is used to implement the electrochemical analytical DPV method to sense the redox current at WE in Potassium Ferricyanide, $K_3[Fe(CN)_6]$ solution. The measured current at the WE is converted to the voltage at the trans-impedance module. The conversion voltage contains negative sign which gives readability limitation to ADC. At the same time, it will lead to signal loss since ADC only read positive voltage values. Thus, level shifter signal conditioning method is used to straighten out these problems. The designed level shifter is expected to attenuate the amplitude of voltage swing in range of 0 to 3.3 V. Therefore the ADC will be able to read the signal from trans-impedance amplifier without truncated.

II. RESEARCH MEHODOLOGY

When Electrochemical cell, analog processing, and digital processing are the three (3) major components of 3 - electrode cell sensing systems used in this potentiostat design. The design of the system and the output waveform for each modules is illustrated in Fig. 2.

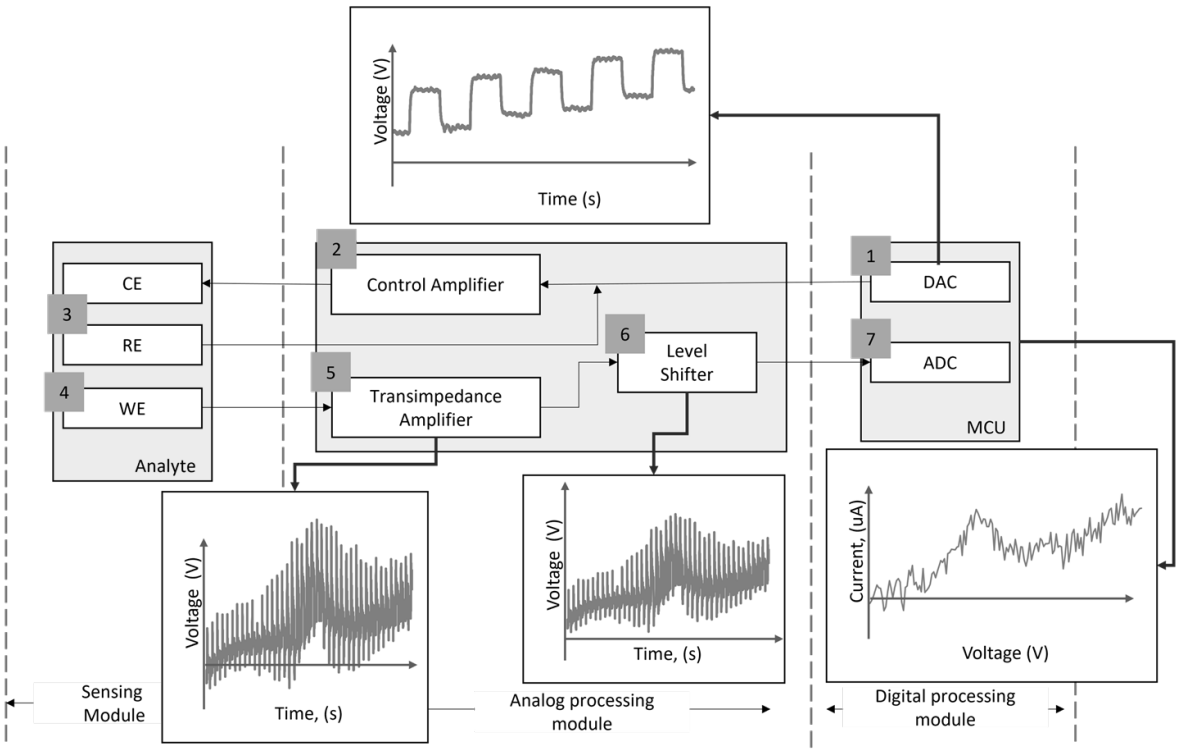

Fig. 2. 3-electrode cell sensing system

A. Sensing Module

In the proposed potentiostat, the sensing module was used to detect the redox reaction. The sensing module consisted of an electrochemical setup that includes electrodes and also an analyte. Three (3) types of electrodes which were counter electrode (CE), reference electrode (RE), and the working electrode (WE) were used in the sensing module. Platinum material with length and diameter of 5.7 and 0.055 cm was used as CE. While, silver/silver chloride (Ag/AgCl) with dimension of 0.078 and 0.006 cm of length and diameter was used as RE. 195 mV of reference potential was provided by RE with an internal solution of 3M NaCl. Meanwhile for WE, a bare gold material with rectangle dimension of 2 x 1 x 0.01 cm was used. 10 mM of $K_3[Fe(CN)_6]$ was used as an analyte sample in this work

B. Analog Processing Module

Several circuitries in the analog processing module was used to control and measure the redox reaction. Each of the modules required the used of op-amp. In this work, AD744JN op-amp type was used. Fig.3 shows the control amplifier circuit which was used in this module to rule the potential applied from Digital Analog Converter (DAC).

Control amplifier consists of two op-amp (OA_1, OA_2), and two resistors (R_1, R_2) values 10 kΩ was used in this work. The negative feedback input (V^-) of OA_1 was swept by a staircase input voltage (V_{in}) received from DAC. The change of V_{in} will affected the voltage potential of WE.

OA_1 was employed to drive the current between CE and WE. CE was utilised to complete the electric circuit, supplying current as well as any voltage required to drive the reaction at

the WE. The solution voltage potential at WE was measured through calculating the potential difference between RE and WE.

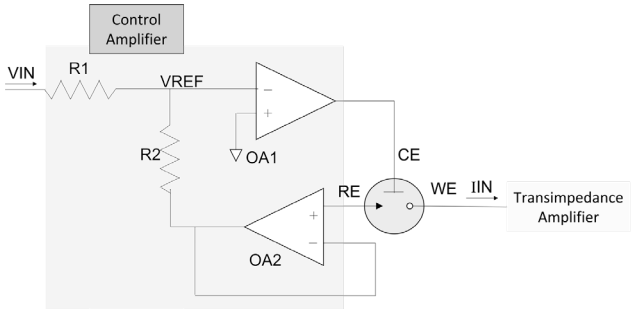

Fig. 3. Control Amplifier Module

While OA_2 was used as voltage follower. OA_2 was connected to RE to secure current from flowing back to OA_1. OA_2 is crucial element that plays two roles which are: as a buffer to the output of RE and supply high input impedance of OA2 respectively.

The potential voltage of OA_1 was kept sufficiently enough to ensure the current flows at the output voltage (Vout) OA_1 and WE are equal. Hence, the potential was able to be maintained at the proper point. RE was used as the potential voltage at V+ of OA_2 since the absent of RE will caused the interference occurs.

As the control amplifier was functioned, the redox reaction at WE was measured by calculating the current flow through OA_3. The measurement of voltage drops across the feedback resistor, R_3 = 5kΩ as shown in Fig.4 will resulting in OA_3 V_{in} = V_{out} / R_3. This circuit configuration was known as a trans-impedance amplifier and capable to convert current in the range of ±500 mA.

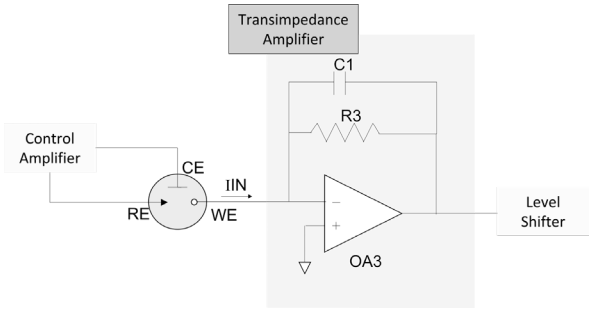

Fig.4. Trans-impedance amplifier module

Due to equipment limitations, trans-impedance amplifier functionality was validated through computer simulation using Multisim software. Input current, I_{in} source was varied from -500 to + 500 mA and V_{out} at OA_3 was observed. From the simulation, the trans-impedance module can convert the current to voltage from ±500 mA to ±2.80 V.

V_{out} produced by OA_3 was passed to the level shifter module for voltage level modification. The function of level shifter is to convert a voltage signal into a significant range for an ADC either by attenuate or amplify the signal. If a direct connection (without a level shifter) is made between output of trans-impedance amplifier to the ADC, the output voltage would cause a loss of signal. This is due to the input voltage ADC is between 0 to 3.3 V. Any values within this range is unable to be read by ADC.

Two types of level shifter were designed and tested for 3-electrode cell redox reaction system compatibility purposed. Fig. 5 shows the first level shifter design which is NSA. This module is a combination of voltage divider circuit and non-inverting summing amplifier circuit. The OA_4 V^+ was connected to voltage divider circuit consist of R_8, R_9 = 20 kΩ, and produced OA_4 V_{out} = 1.65 V which was half of OA_4 V^+. OA_5 V^+ were from the voltage drop of OA_4 V_{out} and trans-impedance amplifier V_{out} at R_7 = 5 kΩ and R_6 = 10 kΩ respectively. The OA_5 V^- was grounded and connected to R_4 = 5 kΩ and R_5 = 10 kΩ. Hence, the trans-impedance amplifier output was scaled down by 0.5 factors through OA_5 with shifted 1.6 V offset level.

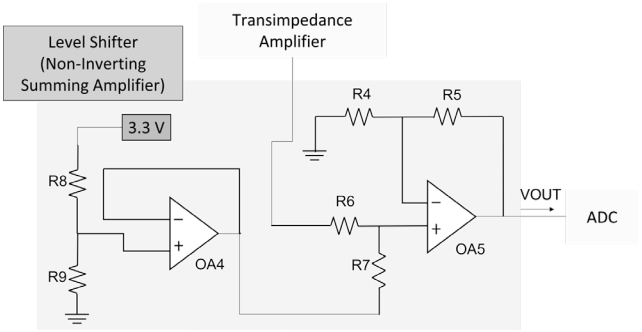

Fig. 5. Non-inverting summing amplifier, NSA

Another level shifter as shown in Fig. 6 namely ISA was designed in this work. OA_4 V_{out} in ISA was similar to the OA_4 in NSA level shifter. V_{out} OA_5 was inverse the V_{in} of it and had gain=1 where R_8 and R_9 are 20 kΩ respectively. OA_6 circuit connections has resulted in amplitude shifting caused by the addition of V_{out} OA_5 and V_{out} trans-impedance amplifier.

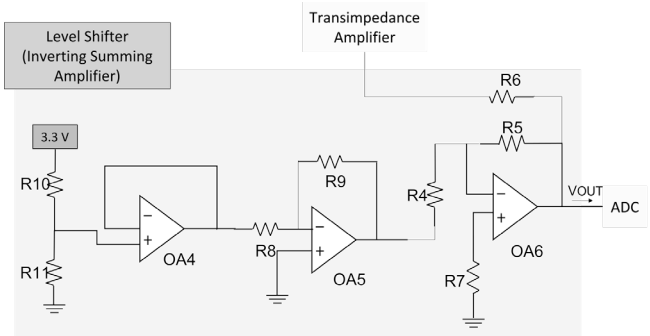

Fig.6. Inverting summing amplifier, ISA

C. Digital Signal Proceessing Module

Digital processing module is the brain of the system for controlling the analog processing and sensing. This module consists of MCU with built-in DAC and ADC respectively. The MCU was programmed to perform DPV electroanalytical

methods in the developed potentiostat. In this method, the applied potential was in a fixed magnitude and linear staircase pulses. The resulting current sampling was done at the end and beginning of each pulse. The difference between these two current samplings were compared and plotted. Thus, resulting in a DPV voltammogram which consists of peak current.

The implementation of DPV was competent to capture the redox reaction through a sensing module and measure it in the analog signal using analog processing module. Besides, the digital processing module was used for level shifter V_{out} conversion. The signal conversion was an important pre-processing step before the signal was sent to MCU. Here, the ADC module is responsible for converting the analog V_{out} of the level shifter into a 12-bit digital signal. For every signal conversion, the data was saved in the MCU's memory. This process was repeated until the final voltage reached. Then, the MCU was programmed to recalculate V_{out} from the level shifter and returned it to the original signal by considering all the involved equations in the circuit. The originality of the redox signals was able to be preserved and therefore the result produced was reliable.

The complete details of circuits involved in this 3-electrode cell redox reaction sensing used in this work is summarized as shown in Fig.7.

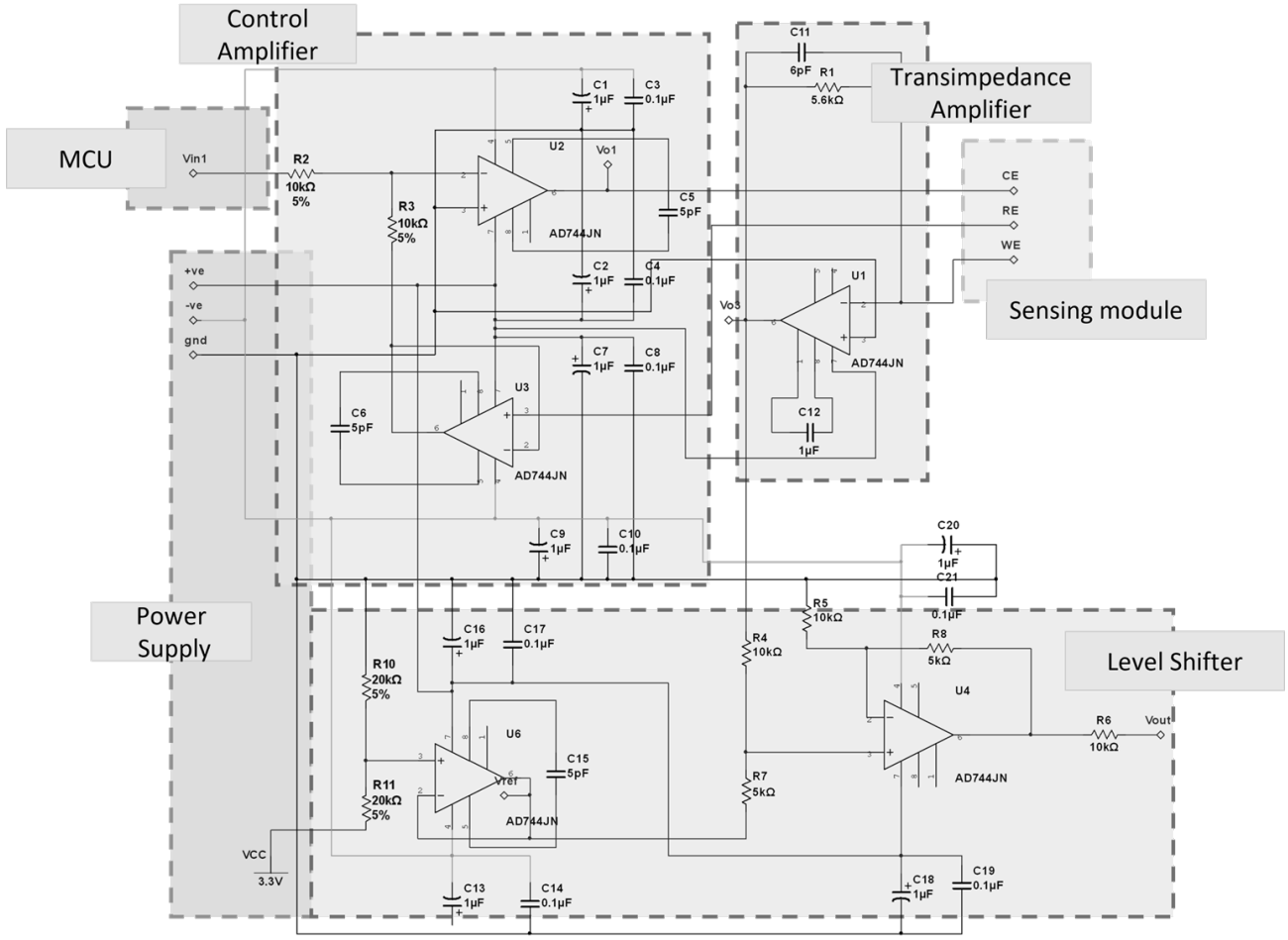

Fig.7. 3-electrode cell redox reaction sensing circuit

III. RESULTS AND DISCUSSION

A. Level Shifter Design Simulation

Fig. 8 shows the comparison of V_{out} from two different types of level shifter design. For both designs, input was set up with peak voltage (V_{peak}) and frequency (f) at 3 V and 1 Hz respectively. Based on Figure 8, the V_{out} for ISA level shifter was shifted to 0.92 V from the original signal while the offset level is was maintained at 0 V. While for NSA level shifter, V_{out} has narrowed down the voltage peak from 3 to 1.65 V. The V_{offset} of NSA level shifter has shifted from 0 to 1.65 V. Based on this result, the NSA level shifter showed an advantage by providing only positive values for the output as the ADC used in this circuit design only support positive values [30].

The obtained results from level shifter in Fig.8 has been tabulated in Table I. From table I, it can be observed that, the minimum voltage (V_{min}) produced by ISA level shifter has exceeded the acceptable voltage limitation of ADC. Technically, the Vout from both designs cannot exceed ADC voltage limitation because it will effect ADC readability and leads to signal loss. Hence, it was concluded that ISA level shifter is less suitable to be used in this 3-electrode redox reaction sensing system.

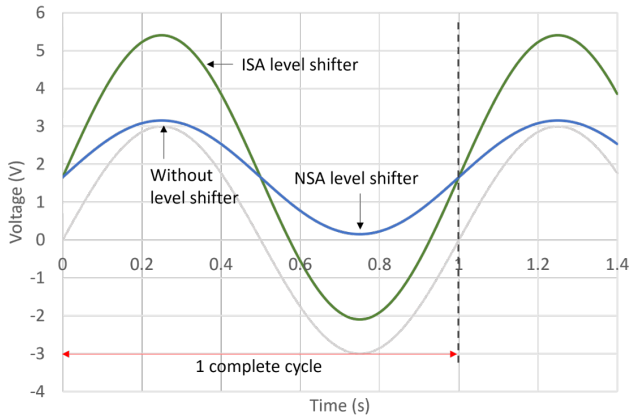

Fig.8. Level shifter design comparison on Vout

TABLE I
SUMMARIZED DATA FOR EACH DESIGN FROM FUNCTION GENERATOR MEASUREMENT

Parameter	V_{max} (V)	V_{min} (V)	V_{pp} (V)	Offset (V)
Input (Function Generator)	3.0	-3.0	6.0	0
ADC	3.3	0	-	-
ISA	5.4	-2.0	7.0	0
NSA	3.0	0	3.0	1.65

Besides that, it also can be observed that the voltage output produced by NSA level shifter gives V_{min} of 0 V same as ADC V_{min} with offset at 1.65 V. Meanwhile, ISA level shifter produced V_{min} of -2.0 V at 0 V offset level. For both designs, ISA level shifter able to amplify the input voltage signal by 1 V larger than original voltage signal while NSA level shifter reduces the voltage half of original voltage signal. By comparing both voltages output produces by NSA and ISA level shifter, it can be said that the NSA level shifter was more suitable for 3-electrode cell redox reaction sensing system because NSA level shifter was able to provide the nearest range of V_{max} and V_{min} compatible to ADC specification.

In order to study the effect of resister values on the output voltage of level shifter, resistance R_4 and R_6 value is varied from 3.3 to 16 kΩ as shown in Fig.9. While R_5 and R_7 is fixed to 5 kΩ. Based on ADC datasheet, the Vout from the level shifter which will be Vin to ADC should be in positive sign value [30]. From the Fig 9, it can be seen that 3.3 kΩ resistance value was saturated at 1st positive cycle and give the negative output voltage at 2nd cycle respectively. While at 5 and 7 kΩ output signal, it can be seen that at 2nd negative cycle of input voltage, the obtained output voltages are ~1.5 and ~0.5 V respectively. Based on the result, the increment value of resistance will narrow down the peak-to-peak output voltage scale.

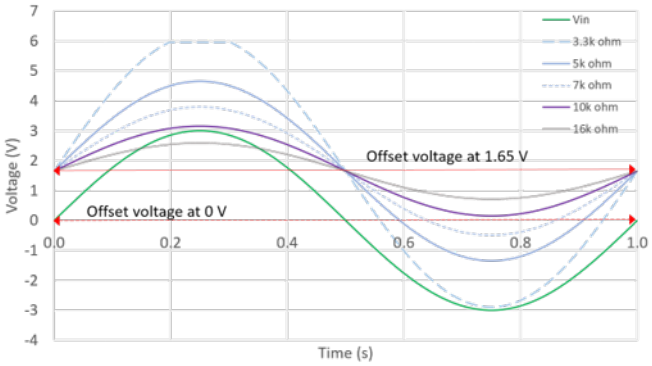

Fig. 9. Effect of input resistance values to the amplitude and offset of output voltage

The effect of resistance values on V_{max}, V_{min}, A_v and V_{pp} were observed and plotted as shown in Fig.10. From Fig.10 resistance value of R_4 and R_6 was inversely proportional to the V_{out}, voltage gain (A_V), and Vpeak-peak (V_{pp}) respectively. A higher resistance value will give a lower V_{out}. Therefore, based on the results obtained in Fig 9 and 10, 10 kΩ resistor shows the excellent results due to optimum potential value and V_{pp} saturated of level shifter obtained using 10 kΩ resistor was nearest to the ADC limitation value (0 V – 3.3V).

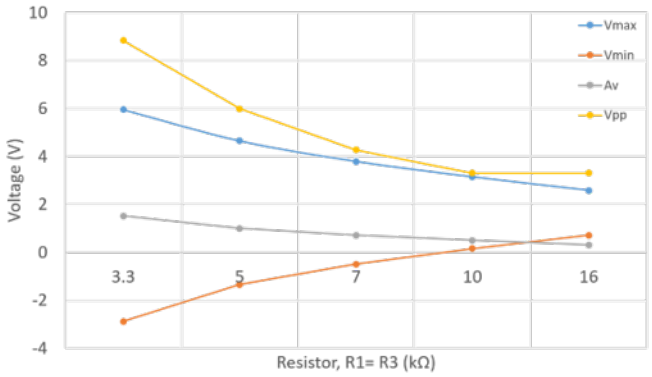

Fig.10. Effect of input resistance values to the V_{max}, V_{min}, A_v and V_{pp}

B. Effect of Level Shifter Design to Differential Pulse Voltammetry (DPV)

In this work, the design of level shifter has also been compared to DPV voltammogram as shown in Fig. 11. From Fig. 11, the DPV voltammogram waveform cannot be produced by MCU without a level shifter module. When a level shifter is added to 3-electrode cell redox reaction sensing system oxidation peak of 138 mV occurs at 5.3 s. While the V_{out} obtained from MCU is around 0.1 to 0.8 V. This shows level shifter plays important role in this system by providing signal readability of the sensing module.

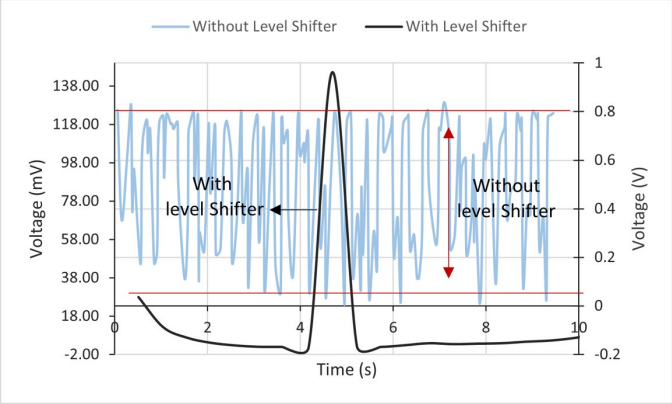

Fig.11. Comparison of Level Shifter effect to the DPV voltammogram

The 3-electrode cell sensing system designed in this work was compared to commercial potentiostat as shown in Fig.12. It can be seen that the corresponding anodic peak current of the $K_3[Fe(CN)_6]$ oxidized at V_{in} at 0.70 V is 81 µA while for commercial potentiostat anodic peak current occur at V_{in} = 0.79 V is 82 µA. Based on this result, the 3-electrode potentiostat design in this work shows only 1.2 % difference compared to commercial potentiostat. Therefore, it can be said that the design potentiostat is comparable to commercial potentiostat.

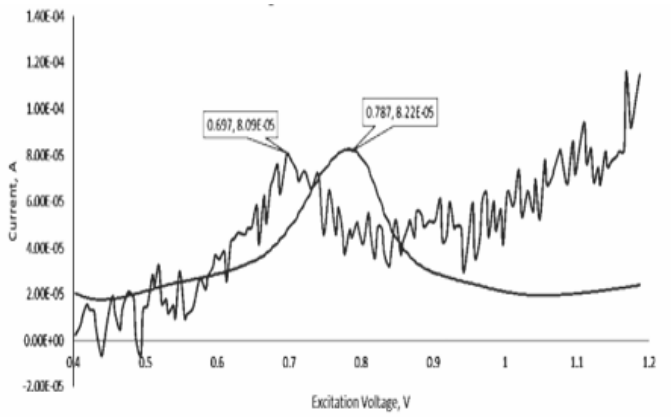

Fig.12. Validation of Differential Pulse Voltammogram for Designed Potentiostat and Commercial Potentiostat

IV. CONCLUSION

The 3-electrode cell potentiostat consisted of 3 main parts: digital, analog, and electrochemical cell parts has been successfully designed. The digital part has the capability to generate a DPV waveform input voltage to the analog part from 0 to 3.3V. The analog part consists of a control amplifier module, trans-impedance module, and a level shifter module respectively. Control amplifier module was a combination of adder and buffer amplifier while the trans-impedance module was a current measurement amplifier. Since ADC cannot accept negative values, 2 types of the level shifter which are non-inverting summing amplifier, NSA, and inverting summing amplifier, ISA were designed and simulated. From the simulation, it was found that the NSA level shifter was more suitable to be used in this system because the voltage produced was fixed to a positive range. The positive output signal was important because the acceptable input voltage conversion of ADC was in a range between 0 - 3.3 V. Besides that, the NSA level shifter was implemented in the 3-electrode cell redox reaction sensing system. It was found out that without NSA level shifter, the system was unable to produce a DPV voltammogram and give a random value between 0.1 V to 0.8 V. By adding the level shifter, the system gives a 25.925 µA oxidation peak at a time of 5.3 seconds. The system was then compared to the standard laboratory potentiostat. The result shows a DPV peak current versus voltage difference of 1.58% and 11.00% respectively. As the percentage difference was insignificant, it can be concluded that the level shifter in the 3-electrode cell redox reaction sensing system was functioning well.

ACKNOWLEDGMENT

This work is funded by the Ministry of Education Malaysia under the Fundamental Research Grant Scheme (Project Code: 600-IRMI/FRGS 5/3 (079/2017).

REFERENCES

[1] A. V. Cordova-Huaman, V. R. Jauja-Ccana, and A. La Rosa-Toro, “Low-cost smartphone-controlled potentiostat based on Arduino for teaching electrochemistry fundamentals and applications,” Heliyon, vol. 7, no. 2, p. e06259, 2021.

[2] Y. Ge et al., “A portable wireless intelligent electrochemical sensor based on layer-by-layer sandwiched nanohybrid for terbutaline in meat products,” Food Chem., vol. 371, p. 131140, 2022.

[3] S. Chinnapaiyan, U. Rajaji, S.-M. Chen, T.-Y. Liu, J. Ilton De Oliveira Filho, and Y.-S. Chang, “Fabrication of thulium metal-organic frameworks based smartphone sensor towards arsenical feed additive drug detection: Applicable in food safety analysis,” Electrochim. Acta, vol. 401, p. 139487, 2022.

[4] S. Khetani et al., “µDrop: Multi-analyte portable electrochemical-sensing device for blood-based detection of cleaved tau and neuron filament light in traumatic brain injury patients,” Biosens. Bioelectron., vol. 178, no. January, p. 113033, 2021.

[5] A. A. Rowe et al., “CheapStat: An Open-Source, ‘Do-It-Yourself’ Potentiostat for Analytical and Educational Applications,” PLoS One, vol. 6, no. 9, p. e23783, Sep. 2011.

[6] D. Sarpong, G. Ofosu, D. Botchie, and F. Clear, “Do-it-yourself (DiY) science: The proliferation, relevance and concerns,” Technol. Forecast. Soc. Change, vol. 158, p. 120127, Sep. 2020.

[7] C. Loncaric, Y. Tang, C. Ho, M. A. Parameswaran, and H.-Z. Yu, “A USB-based electrochemical biosensor prototype for point-of-care diagnosis,” Sensors Actuators B Chem., vol. 161, no. 1, pp. 908–913, Jan. 2012.

[8] Y. Fan et al., “Development of Portable Device for Point-of-Care Testing of Tumor Marker,” Chinese J. Anal. Chem., vol. 44, no. 7, pp. 1148–1154, Jul. 2016.

[9] P. Saha, P. Moitra, U. Bhattacharjee, and S. Bhattacharya, “Selective pathological and intracellular detection of human serum albumin by photophysical and electrochemical techniques using a FRET-based molecular probe,” Biosens. Bioelectron., vol. 203, p. 114007, 2022.

[10] A. G. Ayankojo, R. Boroznjak, J. Reut, A. A. Andres¨opik, and V. Syritski, “Molecularly imprinted polymer based electrochemical sensor for quantitative detection of SARS-CoV-2 spike protein,” Sensors Actuators B. Chem., vol. 353, p. 131160, 2022.

[11] P. Khumwan et al., “Identification of S315T mutation in katG gene using probe-free exclusive mismatch primers for a rapid diagnosis of isoniazid-resistant Mycobacterium tuberculosis by real-time loop-mediated isothermal amplification,” Microchem. J., vol. 175, 2022.

[12] A. A. Rowe et al., “Cheapstat: An open-source, ‘do-it-yourself’ potentiostat for analytical and educational applications,” PLoS One, vol. 6, no. 9, 2011.

[13] W. Gao, X. Luo, Y. Liu, Y. Zhao, and Y. Cui, "Development of an Arduino-based Integrated System for Sensing of Hydrogen Peroxide," Sensors and Actuators Reports, vol. 3, p. 100045, 2021.
[14] S. Abdullah, S. Tonello, M. Borghetti, E. Sardini, and M. Serpelloni, "Potentiostats for protein biosensing: Design considerations and analysis on measurement characteristics," Journal of Sensors, vol. 2019. Hindawi Limited, 2019.
[15] A. Ainla, M. P. S. Mousavi, M. Tsaloglou, J. Redston, G. Bell, and M. T. Ferna, "Open-Source Potentiostat for Wireless Electrochemical Detection with Smartphones," 2018.
[16] C.-Y. Huang, "Design of a Portable Potentiostat with Dual-microprocessors for Electrochemical Biosensors," Univers. J. Electr. Electron. Eng., vol. 3, no. 6, pp. 159–164, Nov. 2015.
[17] M. D. M. Dryden and A. R. Wheeler, "DStat: A Versatile, Open-Source Potentiostat for Electroanalysis and Integration," 2015.
[18] A. Pal, D. Goswami, H. E. Cuellar, B. Castro, S. Kuang, and R. V. Martinez, "Early detection and monitoring of chronic wounds using low-cost, omniphobic paper-based smart bandages," Biosens. Bioelectron., vol. 117, pp. 696–705, Oct. 2018.
[19] S. Bukkawar, N. Sarwade, and M. Panse, "Polyaniline assisted USB based sensor for determination of benzene biomarker," Sens. Bio-Sensing Res., vol. 22, no. November 2018, p. 100260, 2019.
[20] K. Xu, Q. Chen, Y. Zhao, C. Ge, S. Lin, and J. Liao, "Cost-effective, wireless, and portable smartphone-based electrochemical system for on-site monitoring and spatial mapping of the nitrite contamination in water," Sensors Actuators, B Chem., vol. 319, no. April, 2020.
[21] S. D. Adams et al., "A miniature and low-cost glucose measurement system," Biocybern. Biomed. Eng., vol. 38, no. 4, pp. 841–849, 2018.
[22] I. N. Hanitra, F. Criscuolo, N. Pankratova, S. Carrara, and G. De Micheli, "Multichannel Front-End for Electrochemical Sensing of Metabolites, Drugs, and Electrolytes," IEEE Sens. J., vol. 20, no. 7, pp. 3636–3645, 2020.
[23] D. A. Skoog, E. J. Holler, and S. R. Crouch, "Principal Instrumental Analysis Seventh Edition," 7th ed., Boston: Cencage Learning, 2018, pp. 653–694.
[24] S. Toprak, R. Acar Vural, and O. Zafer Batur, "High accuracy potentiostat with wide dynamic range and linearity," Int. J. Electron. Commun., vol. 142, pp. 1434–8411, 2021.
[25] R. W. Shideler and U. Bertocci, "A Low-Noise Potentiostat for the Study of Small Amplitude Signals in Electrochemistry," J. Res. Natl. Bur. Stand. (1934)., vol. 85, no. 3, p. 211, 1980.
[26] V. Bianchi, A. Boni, S. Fortunati, M. Giannetto, M. Careri, and I. De Munari, "A Wi-Fi Cloud-Based Portable Potentiostat for Electrochemical Biosensors," IEEE Trans. Instrum. Meas., vol. 69, no. 6, pp. 3232–3240, 2020.
[27] S. Jeanneret, G. A. Crespo, G. Afshar, and E. Bakker, "GalvaPot, a custom-made combination galvanostat/potentiostat and high impedance potentiometer for decentralized measurements of ionophore-based electrodes," Sensors Actuators B, vol. 207, pp. 631–639, 2015.
[28] R. Pruna et al., "A low-cost and miniaturized potentiostat for sensing of biomolecular species such as TNF-α by electrochemical impedance spectroscopy," Biosens. Bioelectron., vol. 100, pp. 533–540, Feb. 2018.
[29] V. Valente, N. Neshatvar, E. Pilavaki, M. Schormans, and A. Demosthenous, "1.2-V Energy-Efficient Wireless CMOS Potentiostat for Amperometric Measurements," IEEE Trans. Circuits Syst. II Express Briefs, vol. 67, no. 10, pp. 1700–1704, Oct. 2020.
[30] N. Semiconductors, "LPC1769/68/67/66/65/64/63 Product data sheet."